JOURNAL OF SOLID STATE CHEMISTRY 34, 301–313 (1980)

Stereochemically Active $(5s)^2$ Lone Pairs in the Structures of α-InCl and β-InCl

C. P. J. M. VAN DER VORST* AND W. J. A. MAASKANT

Gorlaeus Laboratories, University of Leiden, P.O. Box 9502, 2300 RA Leiden, The Netherlands

Received September 4, 1979

The structures of both the yellow room-temperature (α) and the red high-temperature modification (β) of indium monochloride are interpreted in terms of the stereochemically active $(5s)^2$ lone pair of the monovalent indium ion. A local description is given, in which the pseudo-Jahn–Teller effect $(A_{1g} + T_{1u}) \otimes (t_{1u} + t_{2g})$ of the $InCl_6$ octahedron plays the central role. There are three ways in which a free octahedron with an $(ns)^2$ ion at the center may deform: tetragonal (*a*), digonal (*b*), and trigonal (*c*) in ascending order of stability. α-InCl consists of a rock-salt-like packing of octahedra, roughly of types *b* and *c* (ratio 3 : 5). β-InCl has the β-TlI structure, which may also be derived from a rock salt structure. The coordination polyhedron of the cation shows close relationship to the octahedron of type *a*. Comparison of the $InCl_6$ and $ClIn_6$ octahedra in α-InCl and calculation of the polarization energies of both α- and β-InCl show that the cation polarization is more important than the anion polarization.

1. Introduction

In the class of monohalides of cations with an $(ns)^2$ outer shell all members crystallize in the B2 (CsCl) and/or the B33 (β-TlI) structure, with the exception of tetragonal α-TlF, orthorhombic β-TlF, and yellow α-InCl. The reported structure of α-TlF (*1*) seems unlikely and therefore a new investigation has been undertaken. β-TlF (*2*) has approximately the β-PbO structure, and α-InCl has a unique structure, which was determined for the first time by Van den Berg (*3, 4*). Both β-TlF and α-InCl adopt modified B1 (rock salt) structures. Van der Vorst *et al.* (*5*) redetermined the structure of α-InCl. They also found that the red high-temperature modification, β-InCl, has the B33 structure.

As mentioned α-InCl has a unique structure, which is of extreme complexity. For example, Van den Berg noted the short In–In distances and tried to explain the structure by assuming cation–cation bonding. The structure of β-InCl is, however, not exceptional in the $(ns)^2$ ion halides. The stereochemical activity of the $(ns)^2$ ions has often been described in the literature, e.g., of divalent Pb in β-PbO (*6*). Therefore it seems reasonable to assume that this stereochemical activity plays also a potential role in the structures of β-TlF (with β-PbO structure), of α-InCl, of β-InCl, and of the other compounds in the same class with the B33 structure. In the B2 structure this stereochemical activity seems to be sup-

---

* To whom all correspondence should be addressed.

0022-4596/80/120301-13$02.00/0

pressed as all ions are at a position with an inversion center, although the high dielectric constant may indicate a dynamical effect of the lone pair (*7*).

We first tried to simplify the description of α-InCl by decomposing the deformations in independent normal mode contributions of a B1 structure. There appeared to be five important normal mode components, which was not very elucidating. Probably this is due to the substantial symmetry lowering from $Fm3m$ to $P2_13$. A more fruitful approach is to study the coordination polyhedra of the In^+ ions in the structures of α-InCl and β-InCl. We can show their resemblance with the single octahedra containing a central ion with a lone pair, which have been studied from the viewpoint of crystal field theory by Orgel (*7*) and indirectly by Öpik and Pryce (*8*). A more recent study of the crystal field type on XeF_6 by Wang and Lohr should be mentioned also (*9–11*). A covalent description in VSEPR theory is given by Gillespie (*12–14*) and by Gavin and Bartell (*15*) (Section 2).

One is possibly inclined to underestimate the polarization of cations compared with anions. A reason for this is the generally smaller polarizability of cations. The cations with an $(ns)^2$ configuration, however, are characterized by a larger polarizability, compared with cations of the same ionic radius with a noble gas configuration. This is probably due to the relatively small energy separation between the ^1S and ^1P state (*7*) (Section 2). Although the polarizability of In^+ is not known, we have reason to believe that it is much larger than that of Cl^-. Indeed comparison of anion and cation coordination octahedra in α-InCl indicates that the In^+ is more important than the Cl^- polarization (Section 3). This is also demonstrated by the calculated polarization energies of both α-InCl and β-InCl (Section 4). Section 5 gives the discussion and summary. In particular the hypothesis of Van den Berg on cation–cation bonding will be discussed.

2. Octahedra with an $(ns)^2$ Ion at the Center

2.1. Free Octahedra in the Ionic Picture

Orgel (*7*) considers the possibility of s–p mixing of the $(ns)^2$ lone pair of the B subgroup metal ions under the influence of "ungerade" deformations of their coordination octahedron. If the s and p orbitals were initially degenerate the octahedron would be bound to be distorted, but due to the actual energy separation between s and p orbitals (5–6 eV) it is a quantitative matter to decide whether distortion should occur or not. The author uses a point charge model for his calculations. Because $(ns)^2$ ions have a larger polarizability α compared with ions of the same radius with a noble gas configuration they will show a greater tendency to deform. In order to be distorted the gain in polarization energy, $-\frac{1}{2}\alpha E^2$, where E is the electric field at the central ion, should be greater than the restoring potential of the octahedron. There are many examples of deformed octahedra. Orgel uses the coupling scheme: $(A_{1g} + T_{1u}) \otimes t_{1u}^{\text{stretch}}$. He finds three possible ways for an octahedron to distort:

type a: tetragonal (C_{4v}),
type b: digonal (C_{2v}),
type c: trigonal (C_{3v}),

The deformations have in common that the inversion center is lost.

Öpik and Price (*8*) discuss this problem by introducing the Jahn–Teller instability of the excited ^1P state. The coupling scheme they study is $(A_{1g} + T_{1u}) \otimes (a_{1g} + e_g + t_{2g} + t_{1u}^1 + t_{1u}^2)$, which is composed of the Jahn–Teller effect of the ^1P state, $T_{1u} \otimes (a_{1g} + e_g + t_{2g})$, and the coupling with the ground sate ^1S through the two sets of vibrational modes t_{1u}. Due to the nondegeneracy of the ^1P and ^1S states (which transform in O_h as $^1T_{1u}$ and $^1A_{1g}$, respectively), this is called a pseudo-Jahn–Teller effect. We are interested in their "stationary points of the second kind," which describe deformations with mixed S and P states. They are of three types:

type a: tetragonal (C_{4v}); a_{1g}, t_{1u}, and e_g deformations,

type b: digonal (C_{2v}); a_{1g}, t_{1u}, t_{2g}, and e_g deformations,

type c: trigonal (C_{3v}); a_{1g}, t_{1u}, and t_{2g} deformations.

The two kinds of t_{1u} deformations occur in the same ratio, which implies that there is effectively only one t_{1u} mode. When we neglect the t_{2g} and e_g deformations types a, b, and c are equivalent to Orgel's types a, b, and c, when t_{1u} is a pure stretching mode.

Wang and Lohr (*9–11*) in their study of XeF_6 treat this same problem with crystal field theory. Considering only interaction with a t_{1u} bending mode they arrive at the same types of stationary points, a, b, and c, where the energy is $c < b < a$.

The relative stability of the three types of distortion also seems obvious when one considers the exchange repulsion between the lone pair and the ligands. In the tetragonal kind of distortion the lobe of the lone pair points directly to one ligand. In the digonal kind, b, the lobe points between two ligands, which necessarily form a large edge. And for trigonal deformations the lobe is directed to the center of gravity of a triangle of ligands, which necessarily enlarges. The type a octahedron can be stabilized by removing the most distant ligand, to which the lobe points, or by replacing it with some ligand which leaves more space to the lone pair. Indeed this kind of octahedron usually has no unique sixth group (*7*). If we call the modified version of the type a octahedron type a', we expect the following increase of the exchange repulsion: $a' < c < b < a$. Indium chloride will give proof for this energy criterium.

2.2. Free Octahedron in a Covalent Picture

When the ionic picture fails, either the valence electrons are well localized in regions between the nuclei, or a delocalized model describes the situation. The latter has been suggested for PbS (*16*) and $CsSnBr_3$ (*17, 18*) in order to rationalize the symmetric environment of the $(ns)^2$ ion and the observed metallic properties.

We believe InCl can still be described fairly well by an ionic picture. From microwave rotational spectra the ionicity of molecular InCl was found to be 77% (*19*). However, we want to show in this section that from a more covalent picture the same types of distortions should be expected as for the ionic or the crystal field model.

With a covalent model the concept of hybrid orbitals is often useful (*20*). For example, in the case of a CA molecule, with C a $(ns)^2$ cation (in the ionic picture) and A an anion with noble gas configuration, hybridization of (ns) with the (np) orbital, used for bonding, leads on one hand to a stronger covalent bonding with the anion, and on the other hand to a charge distribution of the lone pair which is no longer centrosymmetrical. The gain in bonding energy has to compete with the hybridization energy.

A second effect also favoring hybridization is the repulsion, both Coulombic and exchange repulsion, between all electron pairs, which tends to keep them as far apart as possible. This is best accomplished when hybrid orbitals are used, as these are off centered. The theory which treats this energy contribution as the most dominant one is the valence shell electron pair repulsion (VSEPR) theory, developed by Gillespie (*12–14*).

Treating the lone pair orbitals and the valence orbitals in $In^+ (Cl^-)_6$ equivalently we have a seven-coordination of electron pairs. This is also the case in XeF_6 with Xe^{6+} a $(5s)^2$ ion. The most probable possibilities for seven-coordination are given by Gillespie (*13*):

I. Octahedron plus extra pair opposite one face.
II. Trigonal prism plus one extra pair opposite the tetragonal face.
III. Pentagonal bipyramide.

Possibilities I and III are especially important in our case: if we place in I the lone pair in the position opposite one face and the bonding pairs in the octahedral positions, we find an octahedron of type *c*. When we place in III the lone pair in one of the planar positions and the bonding pairs with ligands in the other positions, and if we deform the polyhedron further because of the nonequivalence of lone pair and bonding pairs, we arrive at an octahedron of type *b* with a large edge. These two possibilities are also suggested for XeF_6 by Gavin and Bartell (*15*). See also in this respect Refs. (*21–24*). We will show that these two octahedra occur in α-InCl.

A type *a* distortion, with six bonded ligands, is not possible for seven-coordination in the scheme of the VSEPR theory. However, if we do not consider the most distant ligand in an octahedron of type *a* to be bonded, that is, we do not consider it at all (see remark at the end of Section 2.1), then the number of electron pairs in the valence shell is 6. For six-coordination, e.g., in $In^+(Cl^-)_5$, the VSEPR theory predicts an octahedral configuration, which will distort into a type *a'* octahedron because of the nonequivalence of lone pair and valence pair orbitals. This is, e.g., the case in IF_5 (*17*), with I^{5+} an $(5s)^2$ ion. We will show that it also occurs in β-InCl.

We conclude therefore that although the driving forces for deformation are different in the ionic and the covalent picture, both pictures lead roughly to the same types of deformed octahedra: *a'* (with missing sixth ligand), *b*, and *c*, with the lone pair pointing along a fourfold, a twofold, and a threefold axis, respectively. The detailed form of the octahedra depends on the details of the model used. We expect that the energy as a function of all degrees of freedom (t^1_{1u}, t^2_{1u}, t_{2g}, and e_g coordinates) will have a flat well, so that the octahedra of type *a'*, *b*, and *c* are rather flexible. If the single octahedron energy wells are deep enough, the general form of the octahedron may be preserved. This proves to be the case in InCl.

2.3. *The Coordination of In^+ and Cl^- in α-InCl*

The structure of α-InCl, as determined by Van den Berg (*2, 3*) and by Van der Vorst *et al.* (*5*), is a complicated distortion of the B1 structure. The unit cell, which is primitive cubic, has a doubled cell axis (12.373 Å at room temperature) and contains 32 formula units. The space group is $P2_13$, which is a subgroup of index 128 of the space group $Fm3m$ of B1.

There are four different indium species In(1), . . . , In(4) and four different chlorine species Cl(1), . . . , Cl(4). A list of the relative atomic coordinates, together with their deviations from the idealized B1 positions, is given in Table I.

By making models of the coordination octahedra of all four indium ions and all four chlorine ions, we found that there are essentially only two different coordination

TABLE I

RELATIVE ATOMIC POSITIONS AND THEIR DEVIATIONS FROM THE IDEAL POSITIONS IN A B1 STRUCTURE

Ion	Position	x	y	z	x_0	y_0	z_0	δ_x	δ_y	δ_z
In(1)	12*b*	0.2487	0.2198	−0.0288	1/4	1/4	0	−0.0013	−0.0302	−0.0288
In(2)	12*b*	0.7527	0.7781	0.0295	3/4	3/4	0	0.0027	0.0281	0.0295
In(3)	4*a*	0.0302	0.0302	0.0302	0	0	0	0.0302	0.0302	0.0302
In(4)	4*a*	0.4673	0.4673	0.4673	1/2	1/2	1/2	−0.0327	−0.0327	−0.0327
Cl(1)	12*b*	0.3005	−0.0504	0.0005	1/4	0	0	0.0505	−0.0504	0.0005
Cl(2)	12*b*	0.7998	0.0549	−0.0110	3/4	0	0	0.0498	0.0549	−0.0110
Cl(3)	4*a*	0.2061	0.2061	0.2061	1/4	1/4	1/4	−0.0439	−0.0439	−0.0439
Cl(4)	4*a*	0.7986	0.7986	0.7986	3/4	3/4	3/4	0.0486	0.0486	0.0486

Note: Unit of length is a_0 = 12.373 Å.

octahedra of indium, and the same number for chlorine:

$In(1)Cl_6$ is an octahedron roughly of type *b*. We will call it *b*(cation). It has nearly C_2 point symmetry and has a "large" and a "small" edge perpendicular to a pseudo-twofold axis. $In(2)Cl_6$, $In(3)Cl_6$, and $In(4)Cl_6$ are almost equal and are of type *c*. We will call them *c*(cation). They have approximately C_{3v} point symmetry and have "large" and "small" triangles perpendicular to the axis.

For the chlorine coordination octahedra an analogous situation is true:

$Cl(1)In_6$ is a type *b* octahedron, which we will call *b*(anion). Its point group is almost C_2 and it has also "large" and "small" edges perpendicular to its local C_2 axis. $Cl(2)In_6$, $Cl(3)In_6$, and $Cl(4)In_6$ are nearly of identical shape and are of type *c*. We will call this type *c*(anion). There are again "large" and "small" triangles normal to the threefold axis.

All eight-coordination octahedra are given in Figs. 1 and 2, together with the In–Cl, In–In, and Cl–Cl distances. A group theoretical reduction of the deformation of the $InCl_6$ octahedra into their irreducible components of the point group O_h revealed that the deformations consist, apart from translations and rotations, almost entirely of t_{1u} and t_{2g} components. The two sets of t_{1u} vibrations, which are orthogonal to the translation t_{1u} mode, occur each time in almost the same ratio, which is in agreement with the theory of Öpik and Pryce (*8*). The type *b*(cation) has no appreciable e_g components, but instead has a nonnegligible t_{2u} component. Possibly this is a packing effect.

2.4. The Coordination of In^+ in β-InCl

Van der Vorst *et al.* (*5*) found that the red modification of InCl (the β phase), which is stable above 390 K, has the B33 structure. This structure is not uncommon in the class of compounds under study and it is adopted

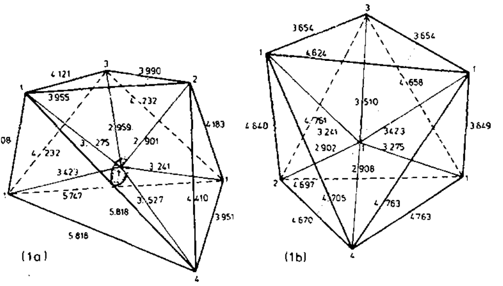

FIG. 1. (a) The $In(1)Cl_6$ octahedron, which is of type *b*(cation). (b) The $Cl(1)In_6$ octahedron of type *b*(anion). The *b*-type octahedra have point group C_1, but "almost" C_2. The In–Cl distances can be divided into three groups: two long, two intermediate, and two short distances. The octahedra have perpendicular to the local pseudo-C_2 axis a "large" edge and a "small" edge. In–In, In–Cl, and Cl–Cl distances are given in the figures. Standard e.s.d's are 0.001, 0.002, and 0.004 Å. The numbers of the crystallographic species are also given.

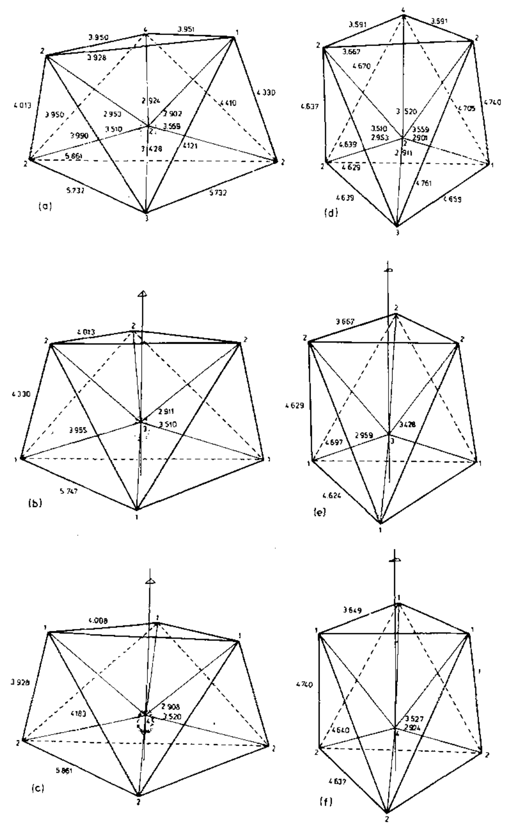

FIG. 2. (a, b, and c) $InCl_6$ octahedra of resp. In(2), In(3), and In(4). They are of type *c*(cation). (d, e, f) $ClIn_6$ octahedra of resp. Cl(2), Cl(3), and Cl(4). They are of type *c*(anion). The point group of crystallographic species 2 is C_1, and that of 3 and 4 is C_3, but all three have almost the same coordination octahedron with pseudosymmetry C_{3v}. The InCl distances can be divided into two groups: three long and three short distances. The octahedra have perpendicular to the C_3 (or pseudo-C_3) axis a "large" triangle and a "small" triangle.

by β-TlI (*25*), InI (*26*), InBr (*27*), and in thin films of TlBr and TlCl (*28*). The B33 structure can be derived from the B1 structure as follows:

(1) First move anion layers, which are perpendicular to a fourfold axis (*z* axis), alternately along this axis. This leads to a double-layer structure, which we will call "B1a," since all cation coordination octahedra are of type *a*. The space group is *P4/nmm*. As marked in Section 2 the type *a* octahedron can be stabilized by removing or replacing the most distant ligand, in order to decrease the exchange repulsion between the lone pair and this ligand. This is done in the second step.

(2) Shear double layers of anions and cations, which are normal to the *z* axis, over a vector $[\frac{1}{4}, \frac{1}{4}, 0]$ relative to each other. We then arrive at the B33 structure with space group *Cmcm*. The lone pair now points toward the middle of a square of two anions and two cations in the neighboring double layer.

In the B33 structure the cation is surrounded by a monocapped trigonal prism of anions, plus the lone pair pointing between two anions of the trigonal prism. This coordination polyhedron is not only found in the B33 structure but also in some coordination complexes of Tl^+ (*29*, *30*). If we do not count the two last-mentioned anions, because they are at the longest distance from the cation, then the coordination polyhedron is an octahedron of type *a'*, with five anions plus a lone pair.

3. Comparison between $InCl_6$ and $ClIn_6$ Octahedra in α-InCl

In Section 2.3 we found that there are essentially two types of In^+ coordination octahedra in α-InCl: *b*(cation) and *c*(cation). With the theories of Sections 2.1 and 2.2 in mind, this is not very surprising, since In^+ is a $(5s)^2$ cation. However, we also found that the coordination octahedra of Cl^-, which has a noble gas configuration, are of types *b* and *c* too. We called them types *b*(anion) and *c*(anion).

There exist differences between the cation octahedra and the anion octahedra of type *c*:

(1) In both *c*(cation) and *c*(anion) there is a "large" and a "small" triangle perpendicular to the main axis. In *c*(cation) the difference in size between "large" and "small"

triangles is more pronounced than in *c*(anion).

(2) In both *c*(cation) and *c*(anion) the central particle is closer to the plane of the "large" triangle than to the plane of the "small" triangle. This difference is more pronounced in *c*(anion) than in *c*(cation). In *c*(cation) the central particle is closer to the ligands which form the "small" triangle, while in *c*(anion) it is closer to the ligands which form the "large" triangle.

(3) The distance between "large" and "small" triangles is shorter in *c*(cation) than in *c*(anion).

(4) The electric field at the central particle, due to the monopoles of its coordination octahedron, consists of a contribution from the "large" and a contribution from the "small" triangle. Both in *c*(cation) and in *c*(anion) the contribution of the "small" triangle dominates. Especially in *c*(cation) the contribution of the "large" triangle is small, due to the larger opening angle with respect to the threefold axis and the relatively long distances between cations and anions. In *c*(anion) the difference between the contributions of "large" and "small" triangles is less pronounced, so that these contributions almost compensate each other. Therefore this electric field at the cation is stronger than the field at the anion by a factor of about 3.

The differences between the cation octahedra and the anion octahedra of type *b* are similar, except that now the emphasis must lie on the "large" and "small" edges perpendicular to the main axis, which is now a pseudo-twofold axis.

In our opinion the agreement between the $InCl_6$ octahedra in α-InCl and the free octahedra, discussed theoretically in Sections 2.1 and 2.2, means that the regular shape of the $InCl_6$ octahedra is due to the properties of the single octahedra. Although the $ClIn_6$ octahedra also have a regular shape, *b*(anion) and *c*(anion), we do not believe that this is caused by the single-octahedron properties in $ClIn_6$. The octahedra in α-InCl are not single octahedra, but they are heavily interconnected. Therefore an interpretation in terms of single octahedra only has validity if the single-octahedron properties are strong enough and are not overwhelmed by packing effects. We think that this is the case with the $InCl_6$ octahedra, but not with the $ClIn_6$ octahedra.

First of all, the electric field, due to the monopoles of the coordination octahedron, is larger on In^+ than on Cl^- (point 4). In case of type *c* octahedra, the electric field direction is due to the "small" triangle. Therefore the direction of this field (e_m^1 in Table II) is toward the "small" triangle of the $InCl_6$ octahedra and toward the "large" triangle of the $ClIn_6$ octahedra. If we take also the monopole contributions of the higher coordination spheres into account, the approximate field direction

TABLE II

APPROXIMATE DIRECTIONS OF THE IONIC SHIFTS AND ELECTRIC FIELDS

Ion	Shift	e_m^1	e_m	e_t
In1	$0\bar{1}\bar{1}$	011	011	011
In2	011	$1\bar{1}\bar{1}$	$1\bar{1}\bar{1}$	$1\bar{1}\bar{1}$
In3	111	$\bar{1}\bar{1}\bar{1}$	$\bar{1}\bar{1}\bar{1}$	$\bar{1}\bar{1}\bar{1}$
In4	$\bar{1}\bar{1}\bar{1}$	111	111	111
Cl1	$1\bar{1}0$	$1\bar{1}0$	$1\bar{1}0$	$\bar{1}10$
Cl2	110	$11\bar{1}$	$0\bar{1}\bar{1}$	$\bar{1}\bar{1}1$
Cl3	$\bar{1}\bar{1}\bar{1}$	$\bar{1}\bar{1}\bar{1}$	111	111
Cl4	111	111	111	$\bar{1}\bar{1}\bar{1}$

Note. The first column gives the ionic species, the position of which is given in Table I. The second column Shift gives the approximate direction, of the ionic shift from the ideal B1 position. See also Table I. The last three columns give the approximate directions of the electric fields on the ions: in the third column is the direction e_m^1 of the monopole field of the first coordination sphere (nearest neighbors); in the fourth column is the direction e_m of the monopole field of the whole crystal; and in the last column is the direction e_t of the total electric field, which is the self-consistent monopole and dipole field of the crystal. The latter two fields are calculated in Section 4.

(see next section) e_m remains the same on In^+, but on Cl(2) and Cl(3) the direction changes considerably. Further the interaction between the dipoles is of importance, especially the influence of the large indium dipoles on the monopole-induced chlorine dipoles. If we take the contribution from the dipoles to the field at an ion into account the field direction (e_t) on In^+ again remains unchanged, while the direction on Cl(1), Cl(2), and Cl(4) changes. Comparison of e_m^1, e_m, and e_t shows that both the packing effects and the influence of the dipolar fields have changed the direction of the electric field on chlorine. The total self-consistent field is even directed opposite to the single-octahedron-monopole field. On the other hand, we may notice that the field directions on indium are equal in all cases. The single-octahedron-monopole field was strong enough and has not changed its direction due to packing effects and dipole–dipole interaction. For the octahedra of type *b* an analogous situation is true.

We do not expect therefore that the regular shape of the $ClIn_6$ octahedra is a "single-octahedron property," but that it is due to other causes. The coherent behavior of the field direction on In^+ and the magnitudes of the field (next section) suggest that the regular shape of the $InCl_6$ octahedra is really a "single-octahedron property."

If we now suppose that the lone pair of indium is pointing into a direction opposite to the electric field ($-e_t$), this means that it points in a type *c* octahedron through the "large" triangle, and in a type *b* octahedron through the "large" edge. This is what we would have expected considering the single coordination octahedra, both on electrostatic grounds ($e_m^1 = e_t$) and because of the minimal exchange repulsion between the lone pair and the ligands.

In Table II we can see that the positive indium ion has not shifted from its ideal position (SHIFT) into the direction of the total field (e_t), which we would have expected at first, but that it has shifted nearly into the direction into which its lone pair fits best (direction $-e_t$; toward the "large" triangle or edge). The negative chlorine ion has shifted into a direction opposite to the electric field, which we would have expected of a negative ion.

4. Calculation of Electric Fields, Madelung Energies, and Polarization Energies

By means of a model in which ions are represented by point charges and coinciding induced point dipole moments $\boldsymbol{\mu} = \alpha \mathbf{E}$ (α = polarizability; $\mathbf{E}$ = total electric field at ion of all other charges and induced dipoles), the potentials and electric fields at the ions were calculated self-consistently. The computer program EWALD (*31*) was used for this purpose. A non-self-consistent calculation, without the inclusion of dipolar fields, was done separately, in order to investigate the influence of dipole–dipole interaction. The calculations were done for both modifications of InCl.

The choice of the values of α is always a problem. The polarizability of Cl^- was taken as 2.96 Å^3 (*32*); the polarizability of In^+ is not known, but is estimated by us at approximately 8 Å^3. This estimation is based upon the known values of α (*32, 33*) of some ions and atoms with an $(ns)^2$ configuration (Table III). In this table one may see that, for $n = 6$, α varies only slightly with the particle charge, as has been discussed by Jørgenson (*34*). We may

TABLE III

POLARIZABILITIES OF SOME IONS AND ATOMS WITH AN $(ns)^2$ CONFIGURATION

$n = 4$ Zn: 6(*33*)	Ga^+: —	Ge^{2+}: —
$n = 5$ Cd: 8(*33*)	In^+: —	Sn^{2+}: —
$n = 6$ Hg: 5.1(*33*)	Tl^+: 5.2(*32*)	Pb^{2+}: 4.9(*32*)

Note. In Å^3; references in parentheses.

expect the same behavior for $n = 5$ and $n = 4$. Thus we have estimates of α which are only dependent on n: for $n = 4$ (Zn, Ga^+, Ge^{2+}) $\alpha = \sim 6$ Å^3; for $n = 5$ (Cd, In^+, Sn^{2+}) $\alpha = \sim 8$ Å^3; and for $n = 6$ (Hg, Tl^+, Pb^{2+}) we see in Table III that $\alpha = \sim 5$ Å^3. The maximum α for $n = 5$, which is found actually for zero particle charge (Zn, Cd, Hg), is probably due to a minimum in the energy gap between the ground state $(ns)^2 - {}^1S_0$ and the excited state $(ns)(np) - {}^1P_1$. This minimum is found for particle charges 0, +1, and +2 (*35*), and can be seen in Table IV. For charges 0 and +1 a minimum for $n = 5$ is also found in the energy of the second important excited state $(ns)((n + 1)p) - {}^1P_1$ (Table IV).

The results of our calculations of the potentials and electric fields in α-InCl can be found in Table V. From this table we can infer that the mean electric monopole field strength on indium (the root mean square or rms value of all In^+ in the cell) is 5.15 times the field strength on chlorine. This factor was about 3 when only the contribution of the coordination octahedron was taken into account (Section 3). Inclusion of the dipolar field has the effect of decreasing the field on indium by 7.8%, and increasing the field on chlorine by 315%, thus reducing the field ratio from 5.15 to 1.14. The changes in the direction of the electric field at chlorine have already been discussed in the previous section. The madelung energy E_{mad}, the part of the polarization energy caused by the monopole fields and dipolar fields, $E^{\mathrm{m}}_{\mathrm{pol}}$ and $E^{\mathrm{d}}_{\mathrm{pol}}$, and the total polarization energy E_{pol} can be derived from the values of Table V, using the following formulas:

$$E_{\mathrm{mad}} = \tfrac{1}{2} \sum_i q_i V^{\mathrm{m}}_i,$$

$$E^{\mathrm{m}}_{\mathrm{pol}} = \tfrac{1}{2} \sum_i \alpha_i \mathbf{E}^{\mathrm{m}}_i \cdot \mathbf{E}^{\mathrm{m}}_i,$$

$$E_{\mathrm{pol}} = \tfrac{1}{2} \sum_i \alpha_i \mathbf{E}_i \cdot \mathbf{E}^{m}_i,$$

$$E^{\mathrm{d}}_{\mathrm{pol}} = E_{\mathrm{pol}} - E^{\mathrm{m}}_{\mathrm{pol}}.$$

TABLE IV

ENERGY GAP $(ns)^2 - {}^1S_0 \rightarrow (ns)(np) - {}^1P_1$ (IN cm^{-1})

$n = 4$ Zn: 46745.37	Ga^+: 70700	Ge^{2+}: 91873
$n = 5$ Cd: 43692.474	In^+: 63033.81	Sn^{2+}: 79911.3
$n = 6$ Hg: 54068.781	Tl^+: 75660	Pb^{2+}: 95340.1

ENERGY GAP $(ns)^2 - {}^1S_0 \rightarrow (ns)((n + 1)p) - {}^1P_1$ (IN cm^{-1})

$n = 4$ Zn: 62910.0	Ga^+: 120540	Ge^{2+}: 184308.8
$n = 5$ Cd: 59905.6	In^+: 109775.39	Sn^{2+}: 162725.1
$n = 6$ Hg: 71295.15	Tl^+: 122379	Pb^{2+}: 177181.4

We find for α-InCl:

$$E_{\mathrm{mad}} = -173.19 \text{ kcal/mole},$$

$$E^{\mathrm{m}}_{\mathrm{pol}} = -25.42 \text{ kcal/mole},$$

$$E^{\mathrm{d}}_{\mathrm{pol}} = +3.52 \text{ kcal/mole},$$

$$E_{\mathrm{pol}} = -21.90 \approx -22 \text{ kcal/mole}.$$

The total electrostatic energy, which is the sum of the madelung and the polarization energy, is:

$$E^{(\alpha\text{-InCl})}_{\mathrm{el.st.}} = -195 \text{ kcal/mole}.$$

This is some 8 kcal/mole lower than the electrostatic energy (madelung energy) of an "ideal InCl structure" of the B1 type with a cell axis of 6.1865 Å, which is −187.46 kcal/mole.

The same calculations have been done for β-InCl. The potentials are given in Table VI. Inclusion of dipolar fields has the effect of increasing the field at In^+ by 18.4% and at Cl^- by 379%, thus reducing the field ratio In : Cl from 3.30 to 0.82. The field at chlorine has changed its direction. With the values of Table VI we find the following energies:

$$E_{\mathrm{mad}} = -174.08 \text{ kcal/mole},$$

$$E^{\mathrm{m}}_{\mathrm{pol}} = -20.05 \text{ kcal/mole},$$

$$E^{\mathrm{d}}_{\mathrm{pol}} = +0.24 \text{ kcal/mole},$$

$$E_{\mathrm{pol}} = -19.81 \approx -20 \text{ kcal/mole},$$

$$E^{(\beta\text{-InCl})}_{\mathrm{el.st.}} = -194 \text{ kcal/mole}.$$

TABLE V

POTENTIALS AND ELECTRIC FIELDS IN α-InCl
Monopole Calculations with Program EWALD

Ion	V^m	E_x^m	E_y^m	E_z^m	E^m	E_{rms}^m
In1	−7.42382	−0.05535	0.93768	1.19972	1.52369	1.97876
In2	−7.55387	1.71549	−1.00769	−1.14333	2.29468	
In3	−7.78951	−0.98131	−0.98131	−0.98131	1.69967	
In4	−7.54152	1.37519	1.37519	1.37519	2.38189	
Cl1	7.41576	0.23426	−0.12646	−0.08000	0.27798	0.38439
Cl2	7.49193	−0.05790	−0.20203	−0.41923	0.46896	
Cl3	7.75918	0.16887	0.16887	0.16887	0.29249	
Cl4	7.49051	0.26134	0.26134	0.26134	0.45266	

Self-Consistent Field Calculations with Program EWALD ($\alpha(In^+) = 8 Å^3$; $\alpha(Cl^-) = 2.96$ Å^3)

Ion	V	E_x	E_y	E_z	E	E_{rms}
In1	−7.96119	0.14034	0.99724	1.33723	1.67402	1.82477
In2	−8.43713	1.40494	−0.65801	−0.90037	1.79373	
In3	−8.03221	−1.31534	−1.31534	−1.31534	2.27824	
In4	−8.64221	1.06279	1.06279	1.06279	1.84080	
Cl1	8.37725	−1.02135	0.91428	0.07992	1.37312	1.59669
Cl2	9.03225	−1.08729	−0.90182	1.06498	1.76908	
Cl3	8.86129	0.76577	0.76577	0.76577	1.32636	
Cl4	8.48205	−1.09404	−1.09404	−1.09404	1.89494	

Note. The potential V is given in Volts; the electric field E in V/Å; the accuracy of computation is 0.005%.

This is only 1 kcal/mole higher than the electrostatic energy of α-InCl. In our calculation the exchange repulsion has not been included so far. In a structure without polarization the exchange repulsion between two ions is often represented by the spherical symmetric Born–Mayer–Huggins expression, which is proportional to $\exp[-(r - r_0)/\rho]$, while the madelung energy is proportional to $-1/r$ (*36*). Minimizing the lattice sum with respect to r shows that the exchange repulsion is a fraction $-\rho/r_0$, which is normally of the order of (10 ± 1)% of the madelung energy. When such a structure, like B1, becomes polarized, the exchange repulsion changes in two ways: First, the polarized ions are no longer spherical, which makes the spherical sym-

TABLE VI

POTENTIALS AND ELECTRIC FIELDS IN β-InCl
Monopole Calculations with Program EWALD

Ion	V^m	E_x^m	E_y^m	E_z^m	E^m
In	−7.60331	0.00000	−1.74042	0.00000	1.74042
Cl	7.50419	0.00000	0.52727	0.00000	0.52727

Self-Consistent Field Calculations with Program EWALD ($\alpha(In^+) = 8$ Å^3; $\alpha(Cl^-) = 2.96$ Å^3)

Ion	V	E_x	E_y	E_z	E
In	−8.18952	0.00000	−2.06101	0.00000	2.06101
Cl	8.63721	0.00000	−2.52778	0.00000	2.52778

Note. The potential V is given in volts; the electric field E in V/Å; the accuracy of computation is 0.001%.

metric exchange potential used a rather crude approximation. In fact the exchange potential should be nonspherical symmetric and dependent upon the polarization state of the ions. In lattice dynamics the shell model is often used for this purpose (*37*, *38*). Second, polarization gives an extra attractive potential between the ions. The main part of this is the interaction between the monopoles and the dipoles, which are induced by the monopoles. This energy term is proportional to $-1/r^4$. In the new stationary state this polarization term is compensated for by extra repulsion energy, of a fraction $4\rho/r_0$ (in the Born–Mayer–Huggins model). This is some 40% of E^{m}_{pol}.

The rest of the polarization energy, E^{d}_{pol}, is mainly an r^{-7} contribution, which leads to an extra exchange interaction of a fraction $7\rho/r_0$ (some 70%).

If we take for ρ the value of 0.345 Å (value for alkali halides (*38*)), and for r_0 the mean distance between nearest neighbors in α-InCl (3.1 Å), then $\rho/r_0 = 11\%$. With these crude figures we can correct the obtained madelung and polarization energies.

$$
\begin{array}{rl}
\alpha\text{-InCl: } E_{mad}\cdot(1-\rho/r_0) & = -154 \text{ kcal/mole} \\
E^{m}_{pol}\cdot(1-4\rho/r_0) & = -14 \text{ kcal/mole} \\
E^{d}_{pol}\cdot(1-7\rho/r_0) & = +1 \text{ kcal/mole} \\
\hline
\text{Sum} & = -167 \text{ kcal/mole} \\
\beta\text{-InCl: } E_{mad}\cdot(1-\rho/r_0) & = -155 \text{ kcal/mole} \\
E^{m}_{pol}\cdot(1-4\rho/r_0) & = -11 \text{ kcal/mole} \\
E^{d}_{pol}\cdot(1-7\rho/r_0) & = +0 \text{ kcal/mole} \\
\hline
\text{Sum} & = -166 \text{ kcal/mole} \\
\text{``Ideal InCl'': } E_{mad}\cdot(1-\rho/r_0) & = -167 \text{ kcal/mole.}
\end{array}
$$

It can be seen that the energies of α-InCl, β-InCl, and "ideal InCl" are equal within the error of the approximation, which amounts to some 2 kcal/mole, because of the inaccuracy in ρ/r_0. Although we did not find that the energies of α-InCl and β-InCl are lower than that of "ideal InCl," owing to the crudeness of the model, we did succeed in showing that the polarization of the indium ion is capable of compensating roughly the difference in madelung energy of the hypothetical "ideal InCl structure" and the two deformed structures, thus showing that the indium polarization is the main source of distortion.

5. Discussion and Summary

In order to interpret the structure of α-InCl, Van den Berg (*3*, *4*), focused attention on the rather short cation–cation distances, which occur in this structure. The shortest distances are 3.591, 3.649, 3.654, and 3.667 Å (*5*). The short In–In distances were ascribed by Van den Berg to covalent bonding between the cations. In our opinion the polarization of the $(5s)^2$ lone pair of the monovalent indium ion is the main source of the deviation of the B1 structure and may explain the short cation–cation distances as well. We summarize the acquired evidence:

(1) In the preceding sections we have shown the resemblance between the cation's coordination octahedra in α-InCl and the free octahedra, studied by Orgel (*7*), by Öpik and Pryce (*8*), and by Gillespie (*9–11*), which are deformed due to the stereochemically active central ion: the octahedra of types *b* and *c* occur in α-InCl. Moreover the octahedron of type *a'*, without the sixth ligand, occurs in β-InCl.

(2) The polarization of the indium ion is also reflected through a change in the exchange repulsion between the cation's deformed electron cloud and its ligands. In Section 2 we mentioned the expected increase of the exchange repulsion between the $(ns)^2$ lone pair and the ligands: $a' < c < b < a$. Because of the increase in volume occupied by the lone pair, we also expect an increase of the exchange repulsion if *n* is increased: $(5s)^2 - In^+ < (6s)^2 - Tl^+$. If the ionic radius of the ligand increases, the exchange repulsion will increase too: $F^- < Cl^- < Br^- < I^-$.

Finally, a temperature increase will, because of the increased vibration amplitudes, also lead to an increase of the exchange repulsion. With this in mind, it is plausible that a compact B1-like structure with type *b* and *c* octahedra occurs only in the low-temperature modification of InCl, and not, e.g., in TlCl or InBr. If the temperature of α-InCl increases, or if the ligand is replaced by a larger one, the α-InCl structure becomes less favorable, and type *a'* has to be used. A B1-like structure with this polyhedron is not possible, but it is found in the less compact B33 double-layer structure, which is a B1 derivative. When In^+ is replaced by Tl^+, the B33 structure is also adopted, but only when at the same time the anion Cl^- is replaced by a sufficiently larger one (I^-): TlCl, TlBr, and high-temperature TlI have the regular B2 structure, in which the stereochemical effect of the lone pair is possibly a dynamical one (*7*). If in InCl the cation In^+ is replaced by the larger Tl^+ and at the same time the anion Cl^- is replaced by a smaller one (F^-) a B1-like structure is again possible: β-TlF or β-PbO. This structure, which also has double layers, contains octahedra which are intermediate between type *a* and type *b*. The derivation of this structure from B1 goes through the hypothetical structure "B1a," mentioned in Section 2.4: In "B1a" anion layers normal to the [100] direction are sheared alternately over a small distance in the [010] direction. This diminishes the exchange repulsion as the lone pair is now not pointing toward the ligand along the *z* axis, but slightly off it.

(3) In the previous section we showed that the polarization energy of both modifications in InCl is capable of compensating the difference in madelung energy of the deformed structures and of the undeformed "ideal InCl" structure. Since the polarization energy is mainly due to indium, the chlorine dipole being induced for the larger part by the indium dipole, we can state that the distortion from a regular B1 structure is due to the tendency of In^+ toward polarization.

(4) Short indium–indium distances arise in α-InCl as a packing effect. If deformed octahedra of types *b* and *c* are stacked in a rock-salt-like way, as in α-InCl, some indium ions may approach each other. As an example, we may mention the building blocks in α-InCl consisting of four edge-coupled octahedra of type *c*. These octahedra share the edges of their "large" triangles in such a way that these triangles form the faces of a large Cl_4 tetrahedron. The lone pair of the indium ion in a *c* octahedron points toward the "large" triangle, and the indium ion itself has shifted in the same direction. Therefore the indium ions point toward the center of the large Cl_4 tetrahedron. They have approached each other and form a small In_4 tetrahedron.

(5) The short In–In distances are at least

8% larger than the shortest distance in In-metal, which is 3.34 Å (*2*).

In conclusion, with regard to the above-mentioned evidence, there is no need to refer to cation–cation bonding at our level of approximation for explaining the structures of indium chloride. We have shown that many features of the structures of α-InCl and β-InCl can be understood by examining the lone pair of the indium ion, which reflects itself through the cation polarization and the exchange repulsion.

Acknowledgments

We thank Dr. J. Basten for his help in the computations with the computer program EWALD, and the Chemistry Department, Rijksuniversiteit Utrecht, for their courtesy in creating these facilities.

References

1. C. Caranoni, R. Favier, L. Capella, and A. Tranquard, *C. R. Acad. Sci. C* **22**, 1795 (1970).
2. N. W. Alcock and H. D. B. Jenkins, *J. Chem. Soc. Dalton Trans.*, 1907 (1974).
3. J. M. Van den Berg, Thesis, University of Leiden (1964).
4. J. M. Van den Berg, *Acta Crystallogr.* **20**, 905 (1966).
5. C. P. J. M. Van der Vorst, G. C. Verschoor, and W. J. A. Maaskant, *Acta Crystalogr. B* **34**, 3333 (1978).
6. J. Galy, G. Meunier, S. Andersson, and A. Åström, *J. Solid State Chem.* **13**, 142 (1975).
7. L. E. Orgel, *J. Chem. Soc.*, 3815 (1959).
8. U. Öpik and F. R. S. Pryce, *Proc. Roy. Soc. Edinburgh A* **238**, 425 (1957).
9. S. Y. Wang and L. L. Lohr, Jr., *J. Chem. Phys.* **60**, 3901 (1974).
10. S. Y. Wang and L. L. Lohr, Jr., *J. Chem. Phys.* **60**, 3916 (1974).
11. S. Y. Wang and L. L. Lohr, Jr., *J. Chem. Phys.* **61**, 4110 (1974).
12. R. J. Gillespie and R. S. Nyholm, *Quart. Rev.* **11**, 339 (1957).
13. R. J. Gillespie, *Canad. J. Chem.* **38**, 818 (1960).
14. R. J. Gillespie, *J. Chem. Educ.* **40**, 295 (1963).
15. R. M. Gavin and L. S. Bartell, *J. Chem. Phys.* **48**, 2466 (1969).
16. H. Krebs, "Fundamentals of Inorganic Crystal Chemistry," 1st ed., p. 186, McGraw-Hill, London (1968).
17. J. D. Donaldson, J. Silver, S. Hadjiminolis, and S. R. Ross, *J. Chem. Soc. Dalton Trans.*, 1500 (1975).
18. S. R. A. Bird, J. D. Donaldson, and J. Silver, *J. Chem. Soc. Dalton Trans.*, 1959 (1972).
19. G. A. Delvigne and H. W. de Wijn, *J. Chem. Phys.* **45**, 3318 (1966).
20. J. E. Huheey, "Inorganic Chemistry: Principles of Structure and Reactivity," Harper & Row New York (1972).
21. D. Britton, *Canad. J. Chem.* **41**, 1632 (1963).
22. T. A. Claxton and G. C. Benton, *Canad. J. Chem.* **44**, 157 (1966).
23. H. B. Thomson and L. S. Bartell, *Inorg. Chem.* **7**, 488 (1968).
24. D. L. Kepert, *Aust. J. Chem.* **31**, 1917 (1978).
25. L. Helmholtz, *Z. Kristallogr. A* **95**, 129 (1936).
26. R. E. Jones and D. H. Templeton, *Acta Crystallogr.* **8**, 847 (1955).
27. N. C. Stephenson and D. P. Mellor, *Aust. J. Sci. Res. A* **3**, 581 (1950).
28. J. Ungelenk, *Phys. Kondens. Mater.* **1**, 152 (1963).
29. P. Jennische and R. Hesse, *Acta Chem. Scand.* **27**, 3531 (1973).
30. H. Pritzkow and P. Jennische, *Acta Chem. Scand.* **A29**, 60 (1975).
31. J. W. Weenk, Thesis, University of Utrecht, Chap. 9 (1976).
32. J. R. Tessman, A. H. Kahn, and W. Shockley, *Phys. Rev.* **92**, 890 (1953).
33. "Landolt-Boernstein Numerical Data," Table 1, Part 1, p. 399; Table 1, Part 3, p. 509, Springer-Verlag, Berlin (1950/1951).
34. C. K. Jørgenson, "Structure and Bonding," Vol. 3, p. 106, Springer-Verlag, Berlin (1967).
35. C. E. Moore, *Nat. Bur. Stand.* (*U.S.*), Circ. No. 467 **1** (1949), **2** (1952), and **3** (1958).
36. M. L. Huggins, *J. Chem. Phys.* **5**, 143 (1937).
37. B. G. Dick and A. W. Overhauser, *Phys. Rev.* **112**, 90 (1953).
38. M. Born and K. Huang, "Dynamical Theory of Crystal Lattices," 1st ed., Chap. 9, Oxford Univ. Press (Clarendon), London (1954).